

# Ister: Inverted Seasonal-Trend Decomposition Transformer for Explainable Multivariate Time Series Forecasting

Fanpu Cao<sup>1</sup>, Shu Yang<sup>2</sup>, Zhengjian Chen<sup>3</sup>, Ye Liu<sup>1</sup>, Laizhong Cui<sup>2</sup>

South China University of Technology<sup>1</sup>, ShenZhen University<sup>2</sup>, Shenzhen Energy Group Co., Ltd.<sup>3</sup>

202164690237@mail.scut.edu.cn, {yangshu, cuilz}@szu.edu.com,  
chenzhengjian@163.com, yliu03@scut.edu.cn

## Abstract

In long-term time series forecasting, Transformer-based models have achieved great success, due to its ability to capture long-range dependencies. However, existing models face challenges in identifying critical components for prediction, leading to limited interpretability and suboptimal performance. To address these issues, we propose the *Inverted Seasonal-Trend Decomposition Transformer (Ister)*, a novel Transformer-based model for multivariate time series forecasting. Ister decomposes time series into seasonal and trend components, further modeling multi-periodicity and inter-series dependencies using a Dual Transformer architecture. We introduce a novel *Dot-attention* mechanism that improves interpretability, computational efficiency, and predictive accuracy. Comprehensive experiments on benchmark datasets demonstrate that Ister outperforms existing state-of-the-art models, achieving up to 10% improvement in MSE. Moreover, Ister enables intuitive visualization of component contributions, shedding lights on model’s decision process and enhancing transparency in prediction results.

## 1 Introduction

Multivariate long-term time series forecasting (LTSF) is widely applied in energy, transportation, economic planning, weather prediction, and disease propagation, and accurate prediction is crucial for them [Wen *et al.*, 2023].

Over the past decades, many statistical models have been proposed, such as Auto Regressive Integrated Moving Average (ARIMA) and its variants [Shumway *et al.*, 2017], while they exhibit poor prediction performance on nonlinear time series datasets. To improve accuracy, various Deep Learning based algorithms have been proposed [Hewage *et al.*, 2020; Grossberg, 2013; Hochreiter and Schmidhuber, 1997]. However, these models perform poorly when predicting extremely long sequences [Zhou *et al.*, 2021].

Due to the significant success of Transformer [Vaswani *et al.*, 2017] in Natural Language Processing, Transformer has recently achieved remarkable success in LTSF [Wen *et al.*, 2023]. Because leveraging the self-attention mechanism,

Transformers effectively capture long-range dependencies in sequences, thereby improving prediction accuracy. However, the vanilla Transformer struggles with accuracy and scalability when directly applied to LTSF. The permutation-invariant nature of self-attention and its insensitivity to sequence order lead to inaccuracies. Furthermore, the quadratic computational complexity of self-attention hinders scalability.

In order to improve the prediction accuracy and computational efficiency of the Transformer-based models, Autoformer [Wu *et al.*, 2021] and FEDformer [Zhou *et al.*, 2022] take *periodic nature* of time series into considerations, and apply Seasonal-Trend decomposition or Fast Fourier Transform (FFT) on long sequence with seasonal characteristics, improving the prediction accuracy.

Unfortunately, a recent paper [Zeng *et al.*, 2023] shows that a simple linear model outperforms previous methods, questioning about the validity of Transformer-based forecasters. The lack of semantic information in individual time steps, combined with embedding multiple variates of the same timestamp into indistinguishable channels, obscures temporal features and leads to the loss of multivariate correlations.

However, since then, many improved Transformer forecasters with Channel Independence architecture have been proposed, and was proved to greatly outperform previous models in the latest benchmark [Liu *et al.*, 2024]. PatchTST [Nie *et al.*, 2023] divides the time series into several segmentations, and apply segmentation-level attention. TimeXer [Wang *et al.*, 2024] integrates endogenous and exogenous information by leveraging patch-wise self-attention and variate-wise cross-attention simultaneously. iTransformer [Liu *et al.*, 2024] embeds series into variate tokens and using a self-attention mechanism to capture *inter-series dependencies*, becoming a milestone in the field.

However, most current Transformer architectures are like ‘black-box’ models, providing minimal interpretability for their predictions. Recent works [Zeng *et al.*, 2023; Liu *et al.*, 2024] indicate that the forecast performance of Transformer-based models varies widely across different types of datasets, with some models underperforming a simple single-layer linear model on specific benchmarks. Additionally, users lack insight into which time series characteristics (e.g., *periodicity* or *inter-series dependencies*) or components the model uses to drive prediction. In real-world applications, characterized by diverse data sources, heterogeneous features, and

significant dataset variability, these challenges are amplified. This significantly increases the effort needed for algorithm optimization, model selection and debugging, making it challenging for users to trust the model’s outputs and impractical to deploy such models in real-world scenarios.

Thus, to better address the previously mentioned issues, we propose a new model named the **Inverted seasonal-trend decomposition Transformer** (*Ister*). *Ister* propose a hierarchical time components decomposition strategy to better capture fine-grained periodic characteristics. Concretely, it firstly decomposes the time-series into seasonal part and trend part, such that periodic information can be learned. Then, in order to capture multi-periodicity, seasonal part is further decomposed into multiple periodic components. By Dual Transformer Blocks, we can capture the multi-periodicity and inter-series dependencies simultaneously, thereby facilitating better prediction. To reduce the computational complexity and provide interpretability, a new *Dot-attention* mechanism is presented. Dot-attention is inspired by the concept of integrated representation, reducing the time complexity to linear through dot product operations. Moreover, it allows users to intuitively visualize the contribution of each local component to the global prediction in the form of a probability distribution, shedding lights on model’s decision process and providing interpretability of the prediction results.

To sum up, the main contributions of this work include:

- Based on the bottleneck of current Transformer-based models, We propose *Ister*, a Transformer model that efficiently identifies critical components for prediction and helps users identify globally-important components for the prediction problem.
- We propose *Dot-attention*, which employs integrated representation, replacing matrix multiplication with element-wise multiplication in self-attention, reducing computational complexity from quadratic to linear.
- We conduct extensive experiments on predicting long multivariate sequences on several real-world benchmarks, and prove that *Ister* outperforms previous methods, achieves state-of-the-art across all of them.

## 2 Related Work

**Transformer Based Methods** Transformer [Vaswani *et al.*, 2017] has achieved remarkable success in NLP and gained significant attention for time series prediction, due to its ability to capture long-range dependencies. Previous works [Kitaev *et al.*, 2020; Zhou *et al.*, 2021; Wu *et al.*, 2021; Zhou *et al.*, 2022] are devoted to reduce quadratic computational complexity in both computation and memory of the vanilla Transformer, while improving its prediction accuracy. However, the point-wise representation performs poorly in capturing local semantics in temporal variations, ultimately leading to a decline in forecasting performance. At the same time, as the sequence length increases, the inference time of Transformer models grows significantly, limiting their practicality.

To improve it, PatchTST [Nie *et al.*, 2023] divides time series data into subseries-level patches and use self-attention to capture dependencies between these patches. iTransformer

[Liu *et al.*, 2024] build upon the inverted embedding structure and tries to capture dependencies between multiple variables. They have been proved to perform better in most scenarios. However, these models often function as black-box systems, making it difficult for users to intuitively determine which characteristics of the time series or components are utilized to aid predictions. Additionally, their performance varies significantly across datasets with different properties, limiting their practical applicability.

**Modeling Periodicity of Time Series** We are not the first to model periodicity of time series. In recent years, Autoformer [Wu *et al.*, 2021] uses auto-correlation to identify sub-series similarities within time series data, FEDformer [Zhou *et al.*, 2022] develops a frequency enhanced Transformer using fourier transform and seasonal-trend decomposition. TimesNet [Wu *et al.*, 2022] unravels intricate frequency patterns using FFT (Fast Fourier Transform) [Brigham and Morrow, 1967] method and explores the multi-periodicity of time series for the first time. However, the patterns captured by these methods often lack semantic information or are obscured by complex weighting operations, hindering clear interpretation of which periodic components are critical to global prediction. We employ a hierarchical approach to divide the time series into distinct, non-overlapping components, effectively capturing multi-periodic characteristics, offering clearer insights into the model’s decision-making process.

## 3 Preliminary

**Problem definition** In multivariate time series forecasting, given historical observations  $\mathbf{X} = \{x_1, \dots, x_T\} \in \mathbb{R}^{T \times N}$ , where  $T$  represents the number of time steps and  $N$  represents the number of variables, our target is predicting the future  $S$  time steps  $\mathbf{Y} = \{x_{T+1}, \dots, x_{T+S}\} \in \mathbb{R}^{S \times N}$ .

**Integrated representation** The DeepSets [Zaheer *et al.*, 2017] is a crucial theoretical tool for processing set-structured data, with extensive applications in deep learning. The core idea of DeepSets is to integrate the information from each element into a unified representation through aggregation.

**Theorem 1** (DeepSets). *Let  $X = \{x_1, x_2, \dots, x_N\}$  be a set of elements where  $x_i \in \mathbb{R}^d$ , and let  $f : 2^{\mathbb{R}^d} \rightarrow \mathbb{R}^m$  be a function operating on the set  $X$ . If  $f$  is permutation-invariant to the input set  $X$ , then  $f$  can be decomposed as:*

$$f(X) = \rho \left( \sum_{x \in X} \phi(x) \right),$$

where  $\phi : \mathbb{R}^d \rightarrow \mathbb{R}^m$  is a learned function that maps each element of the set to an intermediate representation and  $\rho : \mathbb{R}^m \rightarrow \mathbb{R}^m$  is a learned function that aggregates the intermediate representations into the final output.

As previously mentioned, existing methods have difficulty in identifying which components play a major role in the prediction process, limiting the model’s interpretability and application effectiveness. Our goal is to design an algorithm that can automatically identify the core components for prediction and that can provide explanatory properties for the forecasting results. The fusion representation concept in the Theorem 1 has inspired the design of our Dot-attention module.

## 4 Methodology

In this section, we present the overall architecture of the proposed *Inverted Seasonal-Trend Decomposition Transformer (Ister)* (Figure 1). First, we describe the data preprocessing methods in Section 4.1. Then, we introduce Multi-Scale Inverted Embedding in Section 4.2, a channel-independent method for decomposing and embedding time series at multiple scales. Finally, we demonstrate the backbone of Ister (Section 4.3), the Dual Transformer, designed to model both inter-series dependencies and multi-periodicity.

### 4.1 Data Preprocess

**Instance Normalization** Distribution shifts between training and testing datasets are common in time series data [Liu *et al.*, 2022b]. RevIN [Kim *et al.*, 2021] has shown that applying simple instance normalization strategies between the model input and output can effectively mitigate this issue. We use RevIN to eliminate the non-stationary statistics in the input sequence. The RevIN module normalizes the input batch data and denormalizes the output of the model. The instance normalization process corresponds to the Instance Norm and Reverse Norm in Figure 1.

**Series Decomposition** Time series can be decomposed into seasonal and trend components using decomposition algorithm. Seasonal components preserve the periodic features, while trend components depict the overall fluctuations.

To decompose the series into seasonal and trend components, we use a moving average technique to smooth periodic fluctuations and emphasize long-term trends. For an input series  $\mathbf{X} \in \mathbb{R}^{T \times N}$  with  $T$  time steps, the decomposition process is as follows:

$$\mathbf{X}_t = F(\mathbf{X}), \mathbf{X}_s = \mathbf{X} - \mathbf{X}_t \quad (1)$$

where  $F(\cdot)$  is an average pooling filters,  $\mathbf{X}_s$  and  $\mathbf{X}_t \in \mathbb{R}^{T \times N}$  represent the seasonal and extracted trend-cyclical components of  $\mathbf{X}$ , respectively. This process is encapsulated by  $\mathbf{X}_s, \mathbf{X}_t = \text{SeriesDecomp}(\mathbf{X})$ , which serves as an integral component within the model architecture.

As our proposed Ister is designed to focus on multi-periodicity in time-series, we first decompose the input series to obtain the seasonal part, thus removing the interference of the trend part. All subsequent modules of the model keep only the seasonal components involved in the calculations.

### 4.2 Multi-Scale Inverted Embedding

Time series often display distinct multi-periodic patterns. Capturing these patterns requires decomposing the series into segments based on periodicities, explicitly representing the underlying periodic relationships.

Inverted Embedding is a channel-independent approach for high-dimensional embedding along the temporal dimension. This method, validated in [Nie *et al.*, 2023; Liu *et al.*, 2024], has demonstrated effectiveness. Similarly, our proposed model, Ister, employs this embedding approach. We extend its application to embed distinct periodic components of time series, enabling multi-periodic representations of temporal data. Figure 1 and Algorithm 1 illustrates the workflow of Multi-scale Inverted Embedding.

---

#### Algorithm 1 Multi-Scale Inverted Embedding

---

**Input:**  $\mathbf{X} \in \mathbb{R}^{T \times N}$ , where  $T$  is the lookback length, and  $N$  is the number of channels.

**Parameters:**  $k$ : Number of top frequencies.  $D$ : Embedding dimension.

**Variables:**

- $\mathbf{A} \in \mathbb{R}^{T/2}$ : Amplitude of the frequency spectrum.
- $\mathbf{f} = \{f_1, f_2, \dots, f_k\} \in \mathbb{R}^k$ : Selected top- $k$  frequencies.
- $\mathbf{p} = \{p_1, p_2, \dots, p_k\} \in \mathbb{R}^k$ : Period lengths corresponding to  $\mathbf{f}$ .
- $\tau_{i,j} \in \mathbb{R}^{p_i \times N}$ : Subsequence of  $\mathbf{X}$  split by period  $p_i$ .

**Functions:**

- $\text{FFT}(\cdot)$ : Fourier Transform.
- $\text{Amp}(\cdot)$ : Amplitude calculation.
- $\text{TopK}(\cdot, k)$ : Select the top- $k$  values.
- $\text{Padding}(\cdot)$ : Zero-padding to  $T$ .
- $\text{Embedding}(\cdot)$ : Linear projection.
- $\text{Split}(\cdot, p)$ : Divide a sequence into subsequences of length  $p$ .
- $\text{Stack}(\cdot)$ : Stacking operation.
- $\text{Concat}(\cdot)$ : Concatenate operation.

**Output:** Periodic embeddings  $\mathbf{H} \in \mathbb{R}^{(P+1) \times D \times N}$ , where  $P$  is the number of periodic components.

```

1:  $\mathbf{A} = \text{Mean}(\text{Amp}(\text{FFT}(\mathbf{X})))$ 
2:  $\mathbf{f} = \text{TopK}(\mathbf{A}, k)$ 
3:  $\mathbf{p} = \lceil T/\mathbf{f} \rceil$ 
4: for  $i \in \{1, \dots, k\}$  do
5:    $\{\tau_{i,1}, \dots, \tau_{i,j}\} = \text{Split}(\mathbf{X}, p_i), j \in \{1, \dots, \lceil T/p_i \rceil\}$ 
6: end for
7:  $\tau = \text{Stack}(\{\text{Padding}(\tau_{1,1}), \dots, \text{Padding}(\tau_{i,j})\}), \tau \in \mathbb{R}^{P \times T \times N}$ 
8:  $\mathbf{C} = \text{Embedding}(\mathbf{X}), \mathbf{C} \in \mathbb{R}^{D \times N}$ 
9:  $\mathbf{P} = \text{Embedding}(\tau), \mathbf{P} \in \mathbb{R}^{P \times D \times N}$ 
10:  $\mathbf{H} = \text{Concat}(\{\mathbf{C}, \mathbf{P}\})$ 
11: Return  $\mathbf{H}$ .
```

---

The embedding algorithm consists of three main steps. First, FFT is applied to extract periodic information from the frequency domain, segmenting the time series into subsequences based on the top  $K$  prominent periods. Second, these subsequences are padded to a uniform length and embedded into a high-dimensional space using the Inverted Embedding approach. Finally, to preserve the global information required for prediction and to capture inter-series dependencies, the entire sequence is mapped into a high-dimensional space and concatenated with the previously obtained tokens. The obtained tokens are arranged in the order specified in the Algorithm 1 and Figure 1. We summarize the embedding algorithm as follows:

$$\mathbf{H} = \text{MSIE}(\mathbf{X}, k), \mathbf{H} \in \mathbb{R}^{N \times P \times D}$$

where  $\text{MSIE}$  denotes Multi-Scale Inverted Embedding and  $k$  is the hyper-parameter.

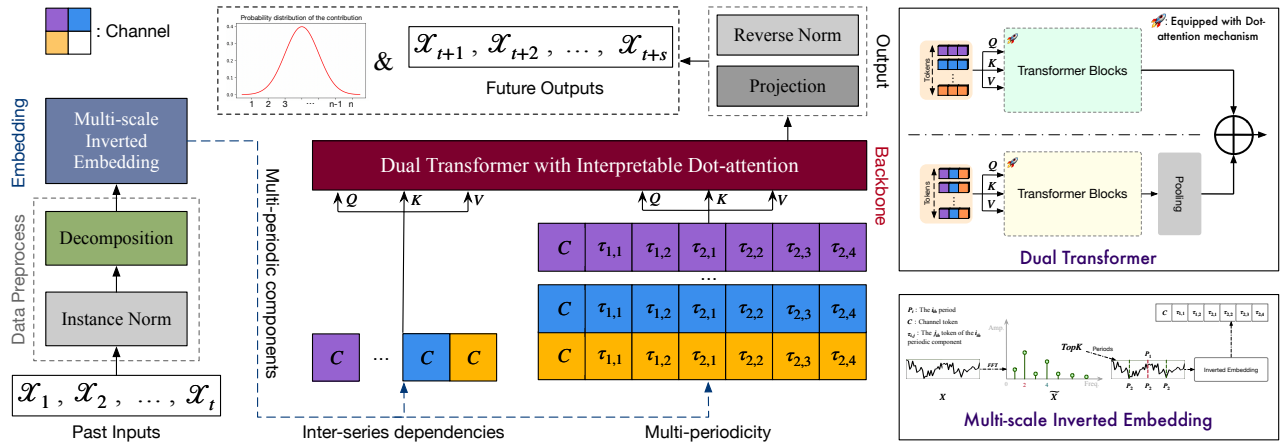


Figure 1: Overall structure of **Ister**. The pipeline of Ister consists of several key stages: data preprocessing, embedding, backbone, and final output. Upon completion of training phase, in addition to generating predictions for future sequences, Ister provides users with the ability to examine the contribution of each component to the final prediction, presented in the form of a probability distribution.

### 4.3 Dual Transformer Backbone

**Dot-attention Mechanism** Previous studies have highlighted the importance of capturing inter-series dependencies to improve prediction accuracy [Liu *et al.*, 2024]. Existing LTSF forecasters rely on the self-attention mechanism to model these dependencies. However, in practical applications, data typically involve a large number of channels, and the quadratic computational complexity of self-attention makes it impractical for long-sequence processing. At the same time, many channels in time-series contain significant noise or lack semantic meaning, making it challenging to manually distinguish the semantic information of each channel. Discarding such channels directly leads to information loss, but excessive modeling may introduce noise, which poses a challenge for accurate prediction.

We examine the state-of-the-art iTransformer [Liu *et al.*, 2024] and find that many channels provide limited information and are excessively noisy, preventing accurate prediction. For example, Figure 2 shows that the attention heat map learned by iTransformer on two well-known datasets [Wu *et al.*, 2021] displays a sparse stripe, suggesting that only a few channels are strongly correlated with the target, while many others play a minimal role in multivariate global prediction. Using self-attention to compute relationships between every pair of channels incurs high computational costs and may introduce noise, potentially degrading performance.

Thus, we argue that not all channels warrant computational resources for precise modeling during channel alignment. Instead, we propose selecting channels that contribute significantly to global prediction and discarding noisy, low-quality channels lacking clear semantic information. Additionally, we aim to quantify each channel’s contribution to global prediction, enhancing the interpretability of model decisions.

In order to solve the bottleneck just mentioned, while improving both efficiency and accuracy, inspired by Theorem 1, we propose *Dot-attention* mechanism. Dot-attention eliminates the multi-head architecture and replaces the matrix multiplication in self-attention with element-wise multiplication.

The formula for Dot-attention is as follows:

$$\text{Dot.}(\mathbf{Q}, \mathbf{K}, \mathbf{V}) = \left( \sum_{i=1}^L \text{Softmax}(\mathbf{Q}_i) \odot \mathbf{K}_i \right)^T \mathbf{1}_L^T \odot \mathbf{V},$$

where  $\mathbf{Q}, \mathbf{K}, \mathbf{V} \in \mathbb{R}^{L \times D}$

(2)

The Dot-attention mechanism, similar to the original multi-head attention mechanism, consists of three learnable weight matrices: 1.  $\mathbf{W}_Q$ : models the importance of different channels and assigns weights to channel information. 2.  $\mathbf{W}_K$ : aggregates the weighted representations of all features into a global predictive representation. 3.  $\mathbf{W}_V$ : using the global predictive representation to guide the predictions for all channels. Specifically, the input tokens are first multiplied by  $\mathbf{W}_Q$ ,  $\mathbf{W}_K$ , and  $\mathbf{W}_V$  to obtain the corresponding representations:  $\mathbf{Q}$ ,  $\mathbf{K}$ , and  $\mathbf{V}$ . A *softmax* operation is then applied to the weight representations, converting each channel’s values into a probability distribution used to scale each channel’s contribution. The weight representation is then multiplied by the global representation via a dot product to extract the core representation of the sequence. Finally, this core representation is multiplied by  $\mathbf{V}$ , which serves as the guide for each channel prediction.

All computational operations of Dot-attention consist of element-wise multiplications. This not only reduces the original quadratic computational complexity of self-attention to  $O(L)$  but also enhancing accuracy. Table 1 lists the time complexities of the existing Transformers. The Dot-attention used by Ister achieves optimal computational efficiency and has the lowest complexity.

At the end of the training phase of Dot-attention, users can input test data into the model and examine the learned weight representations output by the Query matrix. These representations, presented in the form of a probability distribution, quantitatively and transparently measure the contribution of each channel to the global prediction, shed light on the most important components that Ister bases its decisions on.

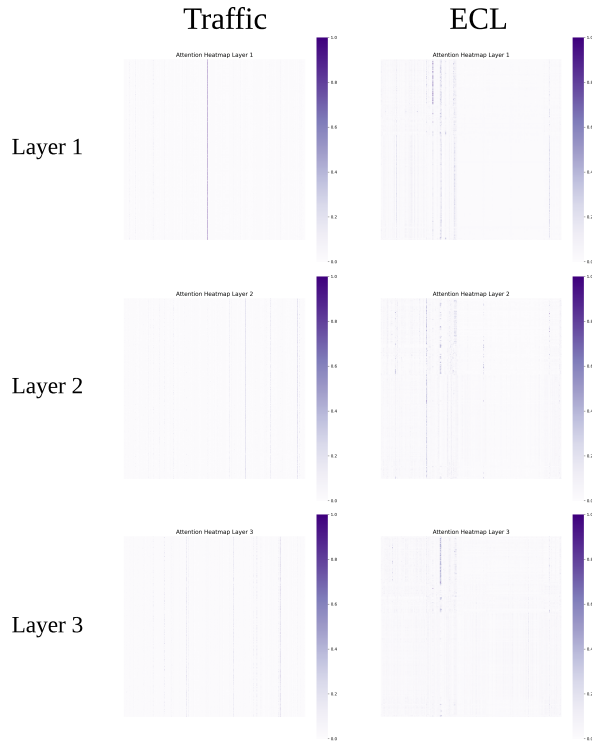


Figure 2: Attention heatmap visualization results of a 3-layer iTransformer after 10 epochs of training on ECL and traffic dataset

**Lemma 1** (Proof is given in Appendix). *If there exist a continuous multivariate function  $f$  that can efficiently captures dependencies between different components, and  $f$  is permutation-invariant to the input set  $X$ , it can be approximated using Dot-attention.*

Model	Attention Algorithm	Complexity
Ister	Dot-attention	$O(L)$
Transformer	Multi-head attention	$O(L^2)$
Reformer	LSH attention	$O(L \cdot \log L)$
Informer	ProbSparse	$O(L \cdot \ln L)$
Autoformer	Auto-Correlation	$O(L \cdot \log L)$
FEDformer	FEA-f	$O(L)$

Table 1: Computational complexities of various algorithms.

**Dual Transformer** *Inter-series dependencies* and *multi-periodicity* are two important characteristics present in time-series. Thus, we propose to use *Dual Transformer* to model these two characteristics simultaneously. Specifically, we design two Transformer modules, each equipped with attention mechanisms tailored for modeling multi-periodic components and channel alignment, respectively.

**Definition 1.** *The token obtained by mapping the entire sequence into a high-dimensional space is referred to as the **Channel token**, denoted as  $\mathbf{C} \in \mathbb{R}^{N \times D}$ . Here,  $N$  represents the number of channels, and  $D$  denotes the hidden dim.*

Using global information from the time series better captures dependencies between channels, as period slices represent only local information and fail to adequately reflect inter-series dependencies. Therefore, only the Channel token, representing global information, is included in the computation when modeling channel alignment.

$$\begin{aligned}
\mathbf{C} &= \mathbf{H}_{:,0,:}, \\
\mathbf{H}' &= \text{Encoder}_H(\mathbf{H}), \\
\mathbf{C}' &= \text{Encoder}_C(\mathbf{C}), \\
\mathbf{H}_{\text{avg}} &= \frac{1}{P} \sum_{p=0}^{P-1} \mathbf{H}'_{:,p,:}, \\
\mathbf{O} &= \mathbf{H}_{\text{avg}} + \mathbf{C}'.
\end{aligned} \tag{3}$$

where  $\mathbf{H} \in \mathbb{R}^{N \times P \times D}$  is obtained using  $MSIE(., k)$ ,  $\mathbf{O}$  denotes the output of the Dual Transformer Blocks, and  $\text{Encoder}_H$  and  $\text{Encoder}_C$  represent the Transformer backbones equipped with Dot-attention, used for modeling multi-periodicity and channel alignment, respectively. We use a simple linear layer to map the output embedding and the trend component to the prediction length. The results are then summed and subjected to an inverse normalization to produce the final prediction.

Dot-attention was originally designed to enhance the performance of capturing inter-series dependencies and improve interpretability. However, empirically, we find that Dot-attention also excels in modeling multi-periodic characteristics, achieving performance comparable to quadratic-complexity multi-head attention mechanisms. Furthermore, due to its inherent interpretability, Dot-attention allows us to analyze the contribution of different periodic components to the final prediction. This not only improves the transparency of the decision-making process but also effectively captures the complex patterns inherent in time-series data.

## 5 Experiment

Our proposed model framework aims to improve performance in LTSF, and we specifically assessed its ability to generalize for these prediction tasks.

**Datasets** We extensively include 6 real-world datasets in our experiments, including ECL, ETT (4 subsets), Exchange, Traffic, Weather used by Autoformer [Wu *et al.*, 2021] and PEMS (4 subsets) used by SCINet [Liu *et al.*, 2022a]. Detailed dataset descriptions are provided in Appendix.

**Setups** For the fairness of the comparison, we set the look-back window for all the methods to 96. Forecast lengths are set to 96, 192, 336, and 720. For PEMS dataset, the forecast lengths are set to 12, 24, 48 and 96. For a detailed analysis of implementation details, please refer to the Appendix.

### 5.1 Forecasting Results

In this section, we conduct extensive experiments to evaluate the forecasting performance of our proposed model together with advanced deep forecasters.

Models	Ister (Ours)		iTransformer [2024]		DLinear [2023]		TimesNet [2022]		PatchTST [2023]		Crossformer [2022]		TiDE [2023]		SCINet [2022a]		FEDformer [2022]		Stationary [2022b]		Autoformer [2021]	
Metric	MSE	MAE	MSE	MAE	MSE	MAE	MSE	MAE	MSE	MAE	MSE	MAE	MSE	MAE	MSE	MAE	MSE	MAE	MSE	MAE	MSE	MAE
ETTm1	<b>0.386</b>	<b>0.399</b>	0.419	0.416	0.403	0.407	0.412	0.418	<b>0.390</b>	<b>0.401</b>	0.594	0.540	0.419	0.419	0.448	0.485	0.481	0.452	0.481	0.456	0.588	0.517
ETTm2	<b>0.279</b>	<b>0.325</b>	0.291	0.333	0.354	0.401	0.296	0.332	<b>0.287</b>	<b>0.330</b>	1.988	0.832	0.358	0.404	0.305	0.349	0.571	0.537	0.306	0.347	0.327	0.371
ETTh1	<b>0.438</b>	<b>0.438</b>	0.463	0.454	0.457	0.451	0.510	0.485	0.447	<b>0.437</b>	0.622	0.573	0.541	0.507	0.747	0.647	<b>0.440</b>	0.460	0.570	0.537	0.496	0.487
ETTh2	<b>0.349</b>	<b>0.387</b>	0.383	0.406	0.562	0.518	0.404	0.419	<b>0.376</b>	<b>0.402</b>	1.894	1.133	0.611	0.550	0.964	0.723	0.437	0.449	0.526	0.516	0.450	0.459
ECL	<b>0.167</b>	<b>0.260</b>	<b>0.179</b>	<b>0.269</b>	0.312	0.407	0.208	0.305	0.204	0.290	0.184	0.281	0.251	0.344	0.268	0.365	0.214	0.327	0.193	0.296	0.227	0.338
Traffic	<b>0.399</b>	<b>0.270</b>	<b>0.421</b>	<b>0.281</b>	0.624	0.383	0.625	0.328	0.502	0.323	0.547	0.298	0.760	0.473	0.804	0.509	0.610	0.376	0.624	0.340	0.628	0.379
Weather	<b>0.243</b>	<b>0.271</b>	0.259	<b>0.279</b>	0.264	0.315	<b>0.258</b>	0.285	0.259	0.280	0.263	0.322	0.271	0.320	0.292	0.363	0.309	0.360	0.288	0.314	0.338	0.382
Exchange	<b>0.352</b>	<b>0.399</b>	0.384	0.418	<b>0.342</b>	0.416	0.411	0.441	0.362	<b>0.401</b>	0.939	0.706	0.447	0.443	0.750	0.626	0.525	0.505	0.551	0.486	0.776	0.578
PEMS03	<b>0.108</b>	<b>0.217</b>	<b>0.113</b>	<b>0.221</b>	0.278	0.375	0.147	0.248	0.180	0.291	0.169	0.281	0.326	0.419	0.114	0.224	0.213	0.327	0.147	0.249	0.667	0.601
PEMS04	<b>0.106</b>	<b>0.213</b>	0.111	0.221	0.295	0.388	0.129	0.241	0.195	0.307	0.209	0.314	0.353	0.437	<b>0.092</b>	<b>0.202</b>	0.231	0.337	0.127	0.240	0.610	0.590
PEMS07	<b>0.092</b>	<b>0.193</b>	<b>0.101</b>	<b>0.204</b>	0.329	0.395	0.124	0.225	0.211	0.303	0.235	0.315	0.380	0.440	0.119	0.234	0.165	0.283	0.127	0.230	0.367	0.451
PEMS08	<b>0.136</b>	<b>0.226</b>	<b>0.150</b>	<b>0.226</b>	0.379	0.416	0.193	0.271	0.280	0.321	0.268	0.307	0.441	0.464	0.158	0.244	0.286	0.358	0.201	0.276	0.814	0.659
1 <sup>st</sup> Count	<b>10</b>	<b>10</b>	0	1	1	0	0	0	0	1	0	0	0	0	1	1	0	0	0	0	0	0

Table 2: Multivariate forecasting results with prediction lengths  $S \in \{12, 24, 36, 48\}$  for PEMS and  $S \in \{96, 192, 336, 720\}$  for others and fixed input sequence length  $T = 96$ . Results are averaged from all prediction lengths. Full results are listed in Appendix.

**Baselines** We carefully choose 10 competitive forecasting models in Long-term Forecasting task as our benchmark, including iTransformer [Liu *et al.*, 2024], DLinear [Zeng *et al.*, 2023], TimesNet [Wu *et al.*, 2022], PatchTST [Nie *et al.*, 2023], Crossformer [Zhang and Yan, 2022], TiDE [Das *et al.*, 2023], SCINet [Liu *et al.*, 2022a] and Non-Stationary Transformer [Liu *et al.*, 2022b].

**Main results** Comprehensive forecasting results are listed in Table 2 with best in **red** and the second in **blue**. The lower MSE/MAE indicates the more accurate prediction result. Previous Transformer-based models fail to achieve optimal performance across all datasets, whereas Ister consistently demonstrates superior predictive performance. Compared to the state-of-the-art iTransformer, our approach achieves a performance improvement of 5% to 10%. Ister is particularly good at forecasting high-dimensional time series, such as the Traffic dataset (862 variables) and the PEMS dataset (170 to 883 variables). This strongly demonstrates that Ister is highly effective in capturing inter-series dependencies, thereby achieving superior performance on multivariate datasets. For datasets with a limited number of variables and strong channel independence (e.g., ETT and Weather), Ister demonstrates excellent predictive performance by effectively capturing multi-periodic patterns in the time series. The experimental results indicate that our model effectively captures critical components contributing to accurate predictions, enabling reliable long-term forecasting and addressing real-world time series scenarios.

## 5.2 Model Analysis

**Ablation study** We conducted ablation experiments on four datasets, including ETT (four subsets), Traffic, Electricity, and Weather, to evaluate the contribution of the two branches in the proposed Dual Transformer: modeling multi-periodicity and modeling inter-series dependencies, to the overall performance improvement. Specifically, ‘w/o Dot.’ represents the removal of all attention modules in the Dual Transformer, ‘+MSA’ means that we replace all Dot-attention modules with Multi-head self attention, ‘w/o periodicity’ and ‘w/o channel-wise’ indicate the removal of the

respective attention modules in each branch. We replace the removed attention module with feed-forward network (FFN) at the corresponding position.

Models	ETT		ECL		Traffic		Weather	
Metric	MSE	MAE	MSE	MAE	MSE	MAE	MSE	MAE
w/o Dot.	0.432	0.447	0.199	0.281	0.499	0.319	0.265	0.283
+MSA	0.368	0.390	0.174	0.268	0.430	0.285	0.248	0.276
w/o channel-wise	0.371	0.393	0.170	0.265	0.456	0.308	0.256	0.279
w/o periodicity	0.411	0.405	0.179	0.287	0.405	0.273	0.248	0.275
Ister (Ours)	<b>0.363</b>	<b>0.387</b>	<b>0.168</b>	<b>0.260</b>	<b>0.399</b>	<b>0.270</b>	<b>0.243</b>	<b>0.271</b>

Table 3: Ablations on Ister. Results are averaged from all prediction length. For ETT dataset, the results are averaged from four datasets {ETTm1, ETTm2, ETTh1, ETTh2}.

As shown in Table 3, both the multi-periodicity modeling and channel-wise alignment contribute significantly to the improvement in predictive performance. Furthermore, the synergistic integration of these two mechanisms further enhances the model’s performance, achieving the optimal results. This demonstrates the effectiveness of the dual modeling approach adopted in the Ister backbone architecture.

In the previous sections, we noted that Dot-attention was originally designed for channel alignment. However, empirical results show that applying Dot-attention to model multi-periodicity also delivers excellent performance. The results in Table 3 indicate that Dot-attention performs comparably to multi-head attention. Furthermore, using Dot-attention to capture multi-periodicity improved computational efficiency and achieved performance gains on several datasets compared to multi-head self attention.

**Interpretability of Dot-attention** To evaluate whether Dot-attention accurately identifies critical time series components and enhances interpretability, we conducted experiments from two perspectives: *channel alignment* and *multi-periodicity*. For channel alignment, experiments were performed on ECL (321 channels) and Traffic (862 channels) datasets with an input-output length of 96-96. For modeling multi-periodicity, we used the ECL and ETTh1 datasets with

an input-output length of 192-48 to better capture periodic characteristics. Figures 3 and 4 visualize the feature representations obtained by the Query matrix’s output.

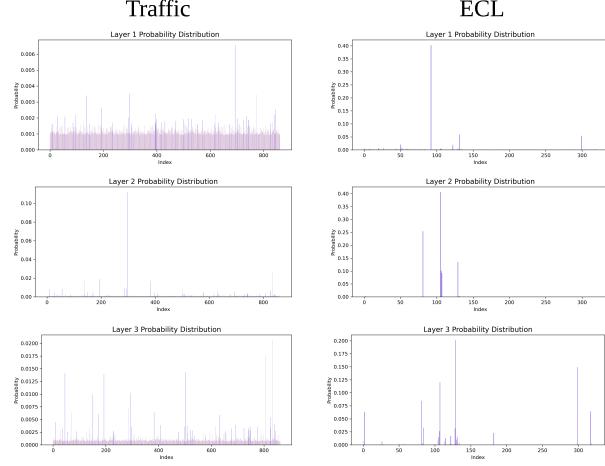


Figure 3: We used a 3-layer Ister trained on ECL and Traffic for 10 epochs and demonstrated the importance of each channel learned by Dot-attention to the overall prediction on the corresponding test set.

Figure 3 shows that for the Traffic and ECL datasets, the weight distribution learned by Dot-attention resembles the attention maps in Figure 2, indicating that a small number of variables significantly contribute to global predictions. This indicates that Dot-attention effectively filters out noise from non-informative channels and identifies key variables essential for prediction. Furthermore, Figure 4 illustrates that Dot-attention captures the contribution of each periodic component and identifies key time slices in the input sequence that significantly impact the forecast. Notably, consistent patterns emerge across different periodic scales. For example, in the ETTh1 dataset, components with periods of 24, 21, and 12 focus on the 120–168 time slice range, indicating that Dot-attention consistently identifies this segment as critical across varying periodic scales. These results demonstrate that Dot-attention accurately identifies core components essential for prediction and offers valuable insights into the model’s decision-making process.

**Generalization performance** We evaluated the generalization performance of *Dot-attention* on other models by selecting three different types of models utilizing self-attention: iTransformer (Channel-wise), PatchTST (Patch-wise), and Transformer (Point-wise). Experiments were conducted on three multivariate datasets: ECL (321 variables), Traffic (862 variables), and PEMS08 (170 variables). Table 4 presents the experimental results and the corresponding percentage improvements. Our findings indicate that *Dot-attention*, which is designed for inter-channel attention, performs well in other tasks as well. It not only retains most of the performance but also achieves improvements in predictive accuracy on certain datasets. The Dot-attention module can be seamlessly integrated into any channel independence Transformer-based model or Linear model, enhancing predictive performance and providing interpretability for the prediction results.

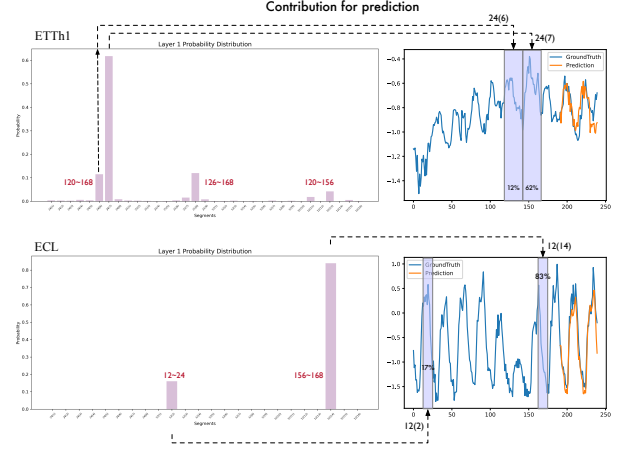


Figure 4: The importance of each period component learned by Dot-attention to the overall prediction. The labels on the x-axis indicate the different periodic components. For example: 24(1) indicates the 1st component obtained by splitting the sequence with a period of 24, and so on. The numbers in red represent the index range of the timing contained in a number of period components.

Models		iTransformer		PatchTST		Transformer	
Metric		MSE	MAE	MSE	MAE	MSE	MAE
ECL	<i>Ori.</i>	0.179	0.269	0.204	0.290	0.414	0.476
	<i>+Dot.</i>	<b>0.172</b>	<b>0.264</b>	<b>0.194</b>	<b>0.288</b>	<b>0.269</b>	<b>0.360</b>
	<i>Promotion</i>	4.0%	2.0%	5.0%	1.0%	35%	25%
Traffic	<i>Ori.</i>	0.412	0.281	0.502	0.323	0.660	0.361
	<i>+Dot.</i>	<b>0.404</b>	<b>0.272</b>	<b>0.450</b>	<b>0.291</b>	<b>0.645</b>	<b>0.359</b>
	<i>Promotion</i>	4.1%	4.3%	11%	10%	2.3%	0.6%
PEMS08	<i>Ori.</i>	0.175	0.254	0.280	0.321	0.252	0.274
	<i>+Dot.</i>	<b>0.169</b>	<b>0.250</b>	<b>0.194</b>	<b>0.263</b>	<b>0.241</b>	<b>0.263</b>
	<i>Promotion</i>	3.5%	1.6%	31%	19%	4.5%	4.0%

Table 4: We compared the performance of original *Multi-head self-attention* and *Dot-attention* for several different types (Channel-wise, Patch-wise and Point-wise) of Transformer models.

## 6 Conclusion and future work

In this paper, we investigate the task of long-term multivariate forecasting of time series, which is a pressing need for real-world applications. To address the lack of interpretability in existing LTSF forecasters, we propose *Ister*, an enhanced Transformer-based model which accurately identifies the core components playing a major role in predictions and provides interpretability for prediction outcomes by simultaneously modeling channel alignment and multi-periodicity in time series. The proposed Dot-attention mechanism improves computational efficiency and predictive accuracy. We conducted experiments on real-world datasets and showed that *Ister* achieves state-of-the-art performance on almost all datasets. Future research will focus on improving *Ister*’s interpretability by providing a clearer rationale for its predictions. Additionally, we will explore more efficient methods to integrate periodicity modeling and channel alignment to further enhance *Ister*’s inference efficiency.

## References

- E. O. Brigham and R. E. Morrow. The fast fourier transform. *IEEE Spectrum*, 4(12):63–70, 1967.
- Abhimanyu Das, Weihao Kong, Andrew Leach, Shaan K Mathur, Rajat Sen, and Rose Yu. Long-term forecasting with tiDE: Time-series dense encoder. *Transactions on Machine Learning Research*, 2023.
- Stephen Grossberg. Recurrent neural networks. *Scholarpedia*, 8(2):1888, 2013.
- Pradeep Hewage, Ardhendu Behera, Marcello Trovati, Ella Pereira, Morteza Ghahremani, Francesco Palmieri, and Yonghuai Liu. Temporal convolutional neural (tcn) network for an effective weather forecasting using time-series data from the local weather station. *Soft Computing*, 24:16453–16482, 2020.
- Sepp Hochreiter and Jürgen Schmidhuber. Long short-term memory. *Neural computation*, 9(8):1735–1780, 1997.
- Taesung Kim, Jinhee Kim, Yunwon Tae, Cheonbok Park, Jang-Ho Choi, and Jaegul Choo. Reversible instance normalization for accurate time-series forecasting against distribution shift. In *International Conference on Learning Representations*, 2021.
- Diederik Kingma and Jimmy Ba. Adam: A method for stochastic optimization. In *International Conference on Learning Representations (ICLR)*, San Diego, CA, USA, 2015.
- Nikita Kitaev, Lukasz Kaiser, and Anselm Levskaya. Reformer: The efficient transformer. In *International Conference on Learning Representations*, 2020.
- Minhao Liu, Ailing Zeng, Muxi Chen, Zhijian Xu, Qiuxia Lai, Lingna Ma, and Qiang Xu. Scinet: Time series modeling and forecasting with sample convolution and interaction. *Advances in Neural Information Processing Systems*, 35:5816–5828, 2022.
- Yong Liu, Haixu Wu, Jianmin Wang, and Mingsheng Long. Non-stationary transformers: Exploring the stationarity in time series forecasting. *Advances in Neural Information Processing Systems*, 35:9881–9893, 2022.
- Yong Liu, Tengge Hu, Haoran Zhang, Haixu Wu, Shiyu Wang, Lintao Ma, and Mingsheng Long. itransformer: Inverted transformers are effective for time series forecasting. In *The Twelfth International Conference on Learning Representations*, 2024.
- Yuqi Nie, Nam H Nguyen, Phanwadee Sinthong, and Jayant Kalagnanam. A time series is worth 64 words: Long-term forecasting with transformers. In *The Eleventh International Conference on Learning Representations*, 2023.
- Adam Paszke, Sam Gross, Francisco Massa, Adam Lerer, James Bradbury, Gregory Chanan, Trevor Killeen, Zeming Lin, Natalia Gimelshein, Luca Antiga, et al. Pytorch: An imperative style, high-performance deep learning library. *Advances in neural information processing systems*, 32, 2019.
- Robert H Shumway, David S Stoffer, Robert H Shumway, and David S Stoffer. Arima models. *Time series analysis and its applications: with R examples*, pages 75–163, 2017.
- Ashish Vaswani, Noam Shazeer, Niki Parmar, Jakob Uszkoreit, Llion Jones, Aidan N Gomez, Łukasz Kaiser, and Illia Polosukhin. Attention is all you need. *Advances in neural information processing systems*, 30, 2017.
- Yuxuan Wang, Haixu Wu, Jiaxiang Dong, Guo Qin, Haoran Zhang, Yong Liu, Yunzhong Qiu, Jianmin Wang, and Mingsheng Long. Timexer: Empowering transformers for time series forecasting with exogenous variables. *arXiv preprint arXiv:2402.19072*, 2024.
- Qingsong Wen, Tian Zhou, Chaoli Zhang, Weiqi Chen, Ziqing Ma, Junchi Yan, and Liang Sun. Transformers in time series: A survey. In Edith Elkind, editor, *Proceedings of the Thirty-Second International Joint Conference on Artificial Intelligence, IJCAI-23*, pages 6778–6786, 8 2023. Survey Track.
- Haixu Wu, Jiehui Xu, Jianmin Wang, and Mingsheng Long. Autoformer: Decomposition transformers with auto-correlation for long-term series forecasting. *Advances in neural information processing systems*, 34:22419–22430, 2021.
- Haixu Wu, Tengge Hu, Yong Liu, Hang Zhou, Jianmin Wang, and Mingsheng Long. Timesnet: Temporal 2d-variation modeling for general time series analysis. In *The eleventh international conference on learning representations*, 2022.
- Manzil Zaheer, Satwik Kottur, Siamak Ravanbakhsh, Barnabas Poczos, Russ R Salakhutdinov, and Alexander J Smola. Deep sets. *Advances in neural information processing systems*, 30, 2017.
- Ailing Zeng, Muxi Chen, Lei Zhang, and Qiang Xu. Are transformers effective for time series forecasting? In *Proceedings of the AAAI conference on artificial intelligence*, volume 37, pages 11121–11128, 2023.
- Yunhao Zhang and Junchi Yan. Crossformer: Transformer utilizing cross-dimension dependency for multivariate time series forecasting. In *The eleventh international conference on learning representations*, 2022.
- Haoyi Zhou, Shanghang Zhang, Jieqi Peng, Shuai Zhang, Jianxin Li, Hui Xiong, and Wancai Zhang. Informer: Beyond efficient transformer for long sequence time-series forecasting. In *Proceedings of the AAAI conference on artificial intelligence*, volume 35, pages 11106–11115, 2021.
- Tian Zhou, Ziqing Ma, Qingsong Wen, Xue Wang, Liang Sun, and Rong Jin. Fedformer: Frequency enhanced decomposed transformer for long-term series forecasting. In *International conference on machine learning*, pages 27268–27286. PMLR, 2022.

## A Dataset decriptions

We conduct experiments on 6 real-world datasets to evaluate the performance of the proposed iTransformer including (1) ETT [Zhou *et al.*, 2021] contains 7 factors of electricity transformer from July 2016 to July 2018. There are four subsets where ETTh1 and ETTh2 are recorded every hour, and ETTm1 and ETTm2 are recorded every 15 minutes. (2) Exchange [Wu *et al.*, 2021] collects the panel data of daily exchange rates from 8 countries from 1990 to 2016. (3) Weather [Wu *et al.*, 2021] includes 21 meteorological factors collected every 10 minutes from the Weather Station of the Max Planck Biogeochemistry Institute in 2020. (4) ECL [Wu *et al.*, 2021] records the hourly electricity consumption data of 321 clients. (5) Traffic [Wu *et al.*, 2021] collects hourly road occupancy rates measured by 862 sensors of San Francisco Bay area freeways from January 2015 to December 2016. (6) PEMS contains the public traffic network data in California collected by 5-minute windows. We use the same four public subsets (PEMS03, PEMS04, PEMS07, PEMS08) adopted in SCINet [Liu *et al.*, 2022a]. You can find all datasets that used by Ister in iTransformer [Liu *et al.*, 2024]’s original paper.

We follow the same data processing and train-validation-test set split protocol used in iTransformer [Liu *et al.*, 2024], where the train, validation, and test datasets are strictly divided according to chronological order to make sure there are no data leakage issues. As for the forecasting settings, we fix the length of the lookback series as 96 in ETT, Weather, ECL, Exchange, Traffic and PEMS, and the prediction length varies in {96, 192, 336, 720}, except for PEMS, where prediction length varies in {12, 24, 48, 96}. The details of datasets are provided in Table 5.

## B Implementation details

All the experiments are implemented in PyTorch [Paszke *et al.*, 2019] and conducted on NVIDIA A800-SXM4-80GB GPUs. We utilize ADAM [Kingma and Ba, 2015] with an initial learning rate in  $\{10^{-3}, 5 \times 10^{-4}, 10^{-4}\}$  and L2 loss for the model optimization. We set the number of Dual Transformer blocks in our proposed model  $L \in \{1, 2, 3, 4\}$ . The dimension of series representations  $D$  is set from {128, 256, 512} and the top- $k$  frequency is set from {2, 3, 4, 5}. All the compared baseline models that we reproduced are implemented based on the benchmark of iTransformer’s Repository [Liu *et al.*, 2024], which is fairly built on the configurations provided by each model’s original paper or official code.

## C Model Analysis

### C.1 Increasing lookback length

Previous works have shown that the forecasting performance does not improve with the increase in lookback length on Transformers [Zeng *et al.*, 2023]. After decomposing time series into seasonal-trend components, as historical information expands, our model can better learn the periodic relationships in temporal data, achieving MSE improvement across multiple prediction steps with increasing lookback window size. The results of the visualization are presented in Figure 5, which proves that Ister can benefit from the extended

---

### Algorithm 2 Ister - Overall Architecture.

---

**Input:** Lookback time series  $\mathbf{X} \in \mathbb{R}^{T \times N}$ .

**Parameter:** input Length  $T$ ; predicted length  $S$ ; variates number  $N$ ; token dimension  $D$ ; Dual Transformer Block number  $L$ .

**Output:** Future time series  $\hat{\mathbf{Y}} \in \mathbb{R}^{S \times N}$ .

```

1:  $\mathbf{X}_s, \mathbf{X}_t = \text{SeriesDecomp}(\mathbf{X})$ 
2:  $\mathbf{X}_s, \mathbf{X}_t = \mathbf{X}_s.\text{transpose}, \mathbf{X}_t.\text{transpose}$ 
3:  $\mathbf{H}^0 = \text{MSIE}(\mathbf{X}_s)$ 
4:  $\mathbf{C}^0 = \mathbf{H}^0_{:,0,:}$ 
5: for  $l \in \{1, \dots, L\}$  do
6:    $\mathbf{H}^{l-1} = \text{Encoder}_H(\mathbf{H}^{l-1})$ 
7:    $\mathbf{C}^{l-1} = \text{Encoder}_C(\mathbf{C}^{l-1})$ 
8: end for
9:  $\hat{\mathbf{H}} = \mathbf{C}^L + \text{Meanpooling}(\mathbf{H}^L)$ 
10:  $\hat{\mathbf{Y}}_s = \text{MLP}(\hat{\mathbf{H}})$ 
11:  $\hat{\mathbf{Y}}_t = \text{MLP}(\mathbf{X}_t)$ 
12:  $\hat{\mathbf{Y}} = \hat{\mathbf{Y}}_s + \hat{\mathbf{Y}}_t$ 
13: Return  $\hat{\mathbf{Y}}$ 

```

---

lookback window for more precise predictions. As can be seen from the figure, the MSE monotonically decreases with increasing length of the lookback window at any prediction length.

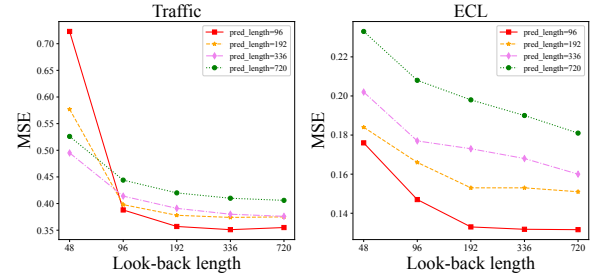


Figure 5: Forecasting performance with the look-back length varying from {48, 96, 192, 336, 720} and prediction length varying from {96, 192, 336, 720}. Different styles of lines represent different prediction lengths. Ister’s forecasting performance benefits from the increase of look-back length.

### C.2 Robustness of Ister

In this section, we evaluate the robustness of Ister through a series of experiments. Specifically, five experiments were conducted using different random seeds, and the averaged results are reported in Table 6. The results demonstrate that Ister consistently achieves robust performance across various datasets and forecasting horizons.

### C.3 Hyper Parameter Analysis

We evaluate the hyperparameter sensitivity of Ister with respect to the following factors:  $k$  for selecting the most important frequency, the number of Transformer blocks  $N$ , and the hidden dimension  $D$ . The results are shown in Figure 6.

Dataset	Dim	Dataset Size	Frequency	Information	Prediction Length
ETTh1, ETTh2	7	(8545, 2881, 2881)	Hourly	Electricity	{96, 192, 336, 720}
ETTm1, ETTm2	7	(34465, 11521, 11521)	15min	Electricity	{96, 192, 336, 720}
Exchange	8	(5120, 665, 1422)	Daily	Economy	{96, 192, 336, 720}
Weather	21	(36792, 5271, 10540)	10min	Weather	{96, 192, 336, 720}
ECL	321	(18317, 2633, 5261)	Hourly	Electricity	{96, 192, 336, 720}
Traffic	862	(12185, 1757, 3509)	Hourly	Transportation	{96, 192, 336, 720}
PEMS03	358	(15617, 5135, 5135)	5min	Transportation	{12, 24, 48, 96}
PEMS04	307	(10172, 3375, 3375)	5min	Transportation	{12, 24, 48, 96}
PEMS07	883	(16911, 5622, 5622)	5min	Transportation	{12, 24, 48, 96}
PEMS08	170	(10690, 3548, 3548)	5min	Transportation	{12, 24, 48, 96}

Table 5: Detailed dataset descriptions. *Dim* denotes the variate number of each dataset. *Dataset Size* denotes the total number of time points in (Train, Validation, Test) split respectively. *Frequency* denotes the sampling interval of time points. *Prediction Length* denotes the future time points to be predicted and four prediction settings are included in each dataset.

Dataset	ECL		ETTh2		Exchange	
Horizon	MSE	MAE	MSE	MAE	MSE	MAE
96	0.138±0.002	0.235±0.000	0.284±0.003	0.341±0.001	0.078±0.002	0.198±0.002
192	0.155±0.002	0.248±0.002	0.355±0.001	0.385±0.001	0.172±0.001	0.298±0.002
336	0.171±0.001	0.265±0.001	0.347±0.002	0.385±0.001	0.320±0.002	0.406±0.001
720	0.203±0.003	0.294±0.001	0.411±0.004	0.438±0.002	0.837±0.030	0.689±0.003
Dataset	PEMS08		Traffic		Weather	
Horizon	MSE	MAE	MSE	MAE	MSE	MAE
96	0.076±0.001	0.174±0.002	0.374±0.003	0.260±0.001	0.157±0.001	0.203±0.000
192	0.106±0.001	0.210±0.002	0.386±0.002	0.265±0.001	0.206±0.001	0.248±0.003
336	0.168±0.000	0.258±0.000	0.405±0.001	0.237±0.002	0.261±0.002	0.290±0.002
720	0.195±0.001	0.264±0.001	0.432±0.001	0.285±0.000	0.346±0.000	0.345±0.001

Table 6: Robustness of Ister performance. The results are obtained from five random seeds.

It’s evident that our proposed Ister exhibits relatively stable performance across different hyperparameter.

#### C.4 Details of Dot-attention Mechanism

To demonstrate how Dot-attention captures core components and contributes to prediction, we analyze its algorithmic details. Assume the time series  $x(t)$  consists of  $N$  components:

$$x(t) = \{x_1(t), x_2(t), \dots, x_N(t)\}.$$

To model the dependencies between these components, Dot-attention operates over the components as follows:

$$Q_i = W_Q x_i(t), \quad K_i = W_K x_i(t), \quad V_i = W_V x_i(t),$$

where  $W_Q$ ,  $W_K$ , and  $W_V$  are learnable weight matrices. The output is computed as:

$$\text{Dot.}(\mathbf{Q}, \mathbf{K}, \mathbf{V}) = \left( \sum_{i=1}^N \text{Softmax}(\mathbf{Q}_i) \odot \mathbf{K}_i \right)^\top \mathbf{1}_N^\top \odot \mathbf{V},$$

resulting in an updated representation of the time series components. The input-output relationship can be summarized as:

$$\{\hat{x}_1, \hat{x}_2, \dots, \hat{x}_N\} = \text{Dot.}(\{x_1, x_2, \dots, x_N\}).$$

#### Proof of Dot-attention Representation

We formally show that Dot-attention aligns with the DeepSets representation theorem.

*Proof.* Assume  $x = \{x_1, x_2, \dots, x_N\}$ . The weight representation for each component is:

$$g(x_i) = \text{Softmax}(W_Q x_i) = \frac{e^{W_Q x_i}}{\sum_{j=1}^N e^{W_Q x_j}}.$$

Dot-attention can then be expressed as:

$$\text{Dot.}(\{x_1, \dots, x_N\}) = \left( \sum_{i=1}^N g(x_i) \odot K_i \right)^\top \mathbf{1}_N^\top \odot V.$$

Simplifying further:

$$\text{Dot.}(\{x_1, \dots, x_N\}) = V \left( \sum_{i=1}^N K_i g(x_i) \right).$$

Let  $y_i = g(x_i)$ , and define  $h(y_i) = K_i y_i$  and  $\rho(x) = Vx$ . Then:

$$V \left( \sum_{i=1}^N K_i g(x_i) \right) = \rho \left( \sum_{i=1}^N h(y_i) \right).$$

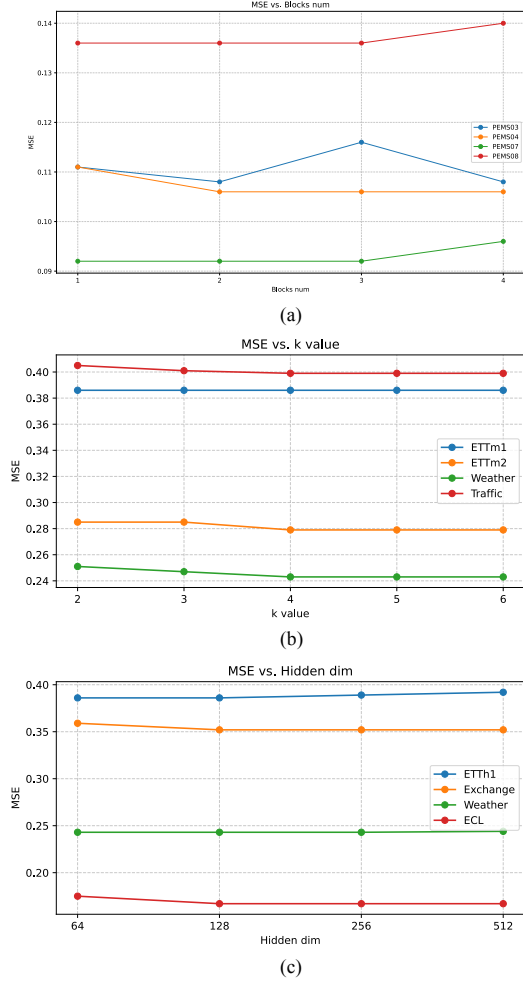


Figure 6: Sensitivity analysis of hyper-parameters.

The Dot-attention formulation now aligns with the DeepSets representation theorem. Regarding channel alignment, since different channel data are aggregated, disordered, and permutation-invariant, their arrangement does not affect performance. However, the relationship between multi-periodic components is different from that between channels, as each component depends on the temporal sequence order. Alignment modeling with permutation-invariant algorithms may result in information loss. However, experimental evidence shows that Dot-attention still performs well in modeling multi-periodicity. This may be because a subset of core components strongly dominates the prediction, enabling excellent performance even without modeling dependencies between components.  $\square$

## C.5 Model Limitations and Future work

**Model efficiency** We propose Ister, which accurately identifies key components and provides interpretability for prediction results, while reducing the primary computational bottleneck in Transformers—namely, the quadratic complexity of attention—to linear. However, due to the Dual Transformer architecture requiring two forward passes for the input tokens, the overall computational overhead remains significant. However, since Dot-attention has linear complexity and utilizes Inverted-embedding to extract temporal information, our model’s memory usage is less dependent on the prediction horizon compared to other Transformer-based methods, where memory usage increases linearly with the prediction horizon. In contrast, iTransformer’s computational overhead increases quadratically with the number of channels due to its attention mechanism, whereas Ister scales linearly. This ensures **superior scalability** when handling larger datasets.

**Compatibility between channel alignment and multi-periodicity** Through extensive offline experiments, we observed that inter-series dependencies and multi-periodicity cannot be effectively integrated within a single Transformer block solely by stacking attention mechanisms. Furthermore, the effectiveness of these features is constrained by the nature of the data itself—for instance, multi-periodicity modeling performs better for data with strong channel independence, whereas channel alignment is more advantageous for data with strong inter-channel correlations. In future work, we aim to develop more efficient architectures that can simultaneously accommodate both characteristics while improving the model’s inference efficiency.

## D Visualization of prediction results

To provide a clear comparison among different models, we list supplementary prediction showcases of four representative datasets in Figures, which are given by the following models: Ister, iTransformer [Liu *et al.*, 2024], DLinear [Zeng *et al.*, 2023], TimesNet [Wu *et al.*, 2022], PatchTST Nie *et al.* [2023] and Crossformer [Zhang and Yan, 2022]. Among the various models, Ister predicts the most precise future series variations and exhibits superior performance.

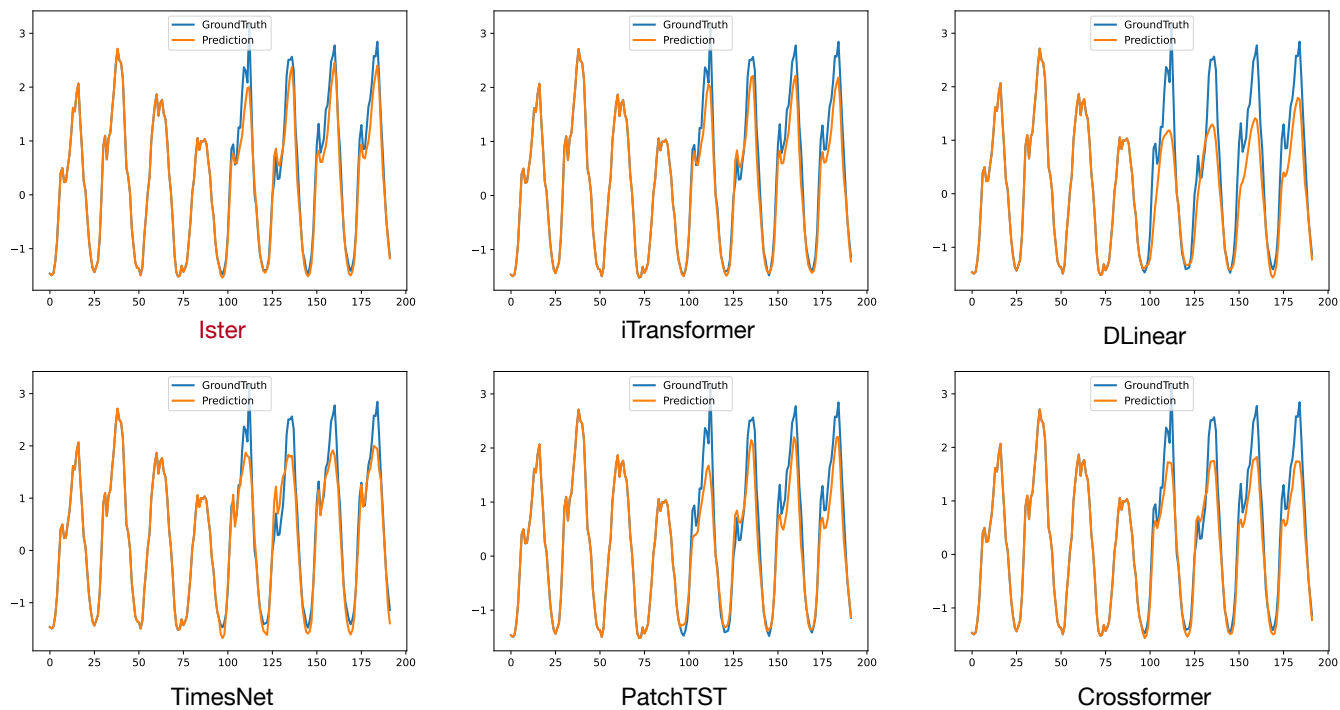


Figure 7: Visualization of input-96-predict-96 results on the Traffic dataset.

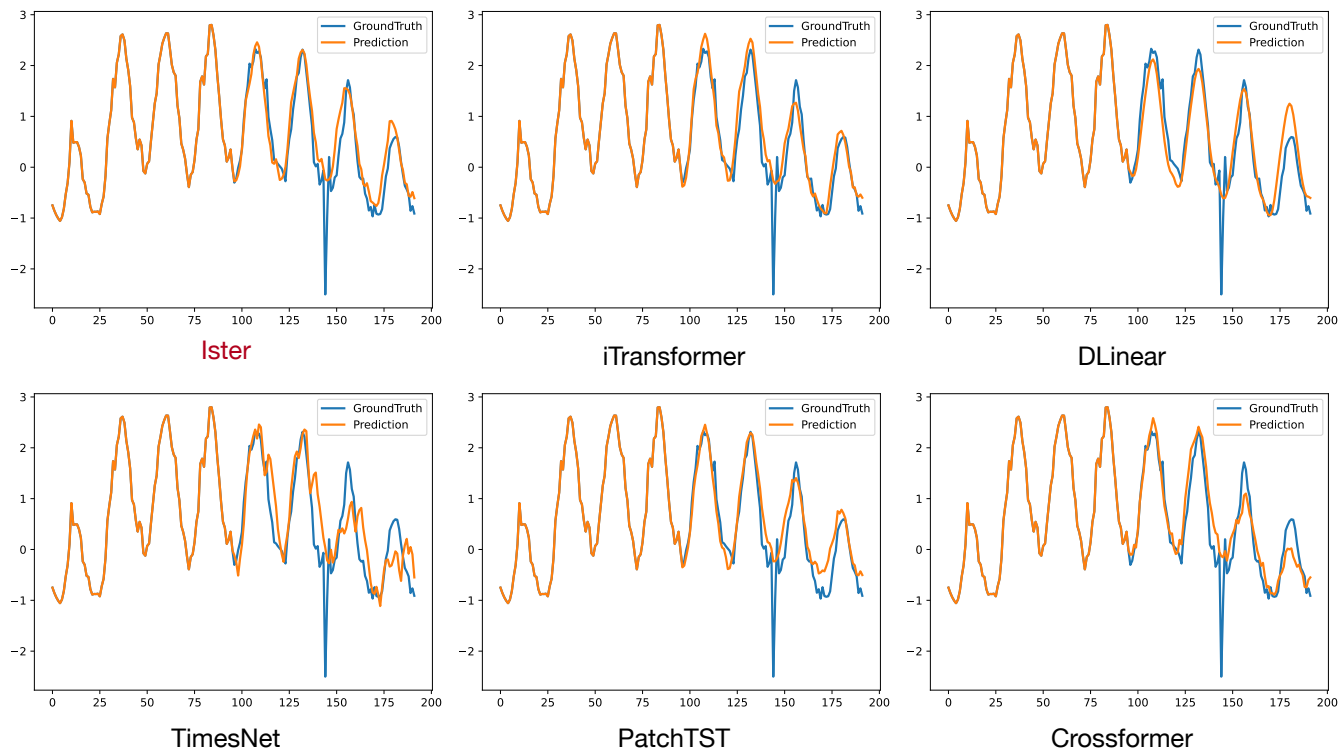


Figure 8: Visualization of input-96-predict-96 results on the ECL dataset.

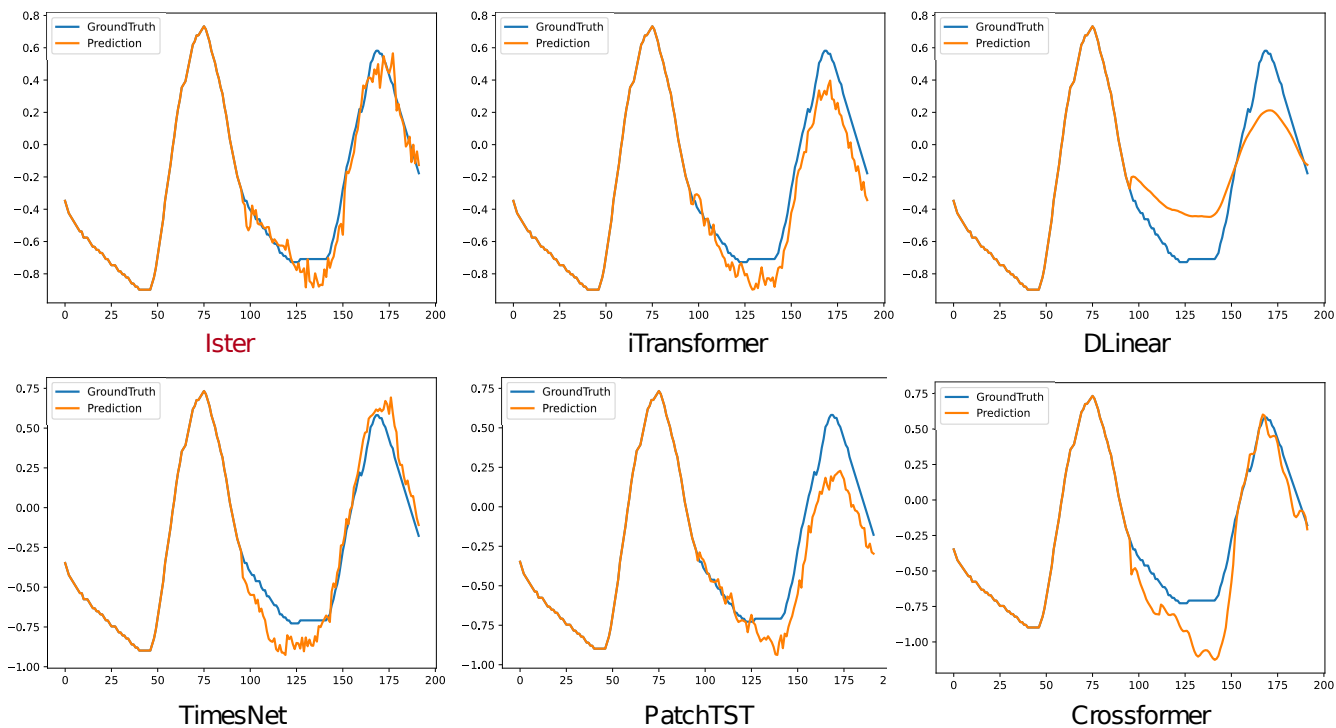


Figure 9: Visualization of input-96-predict-96 results on the ETTm2 dataset.

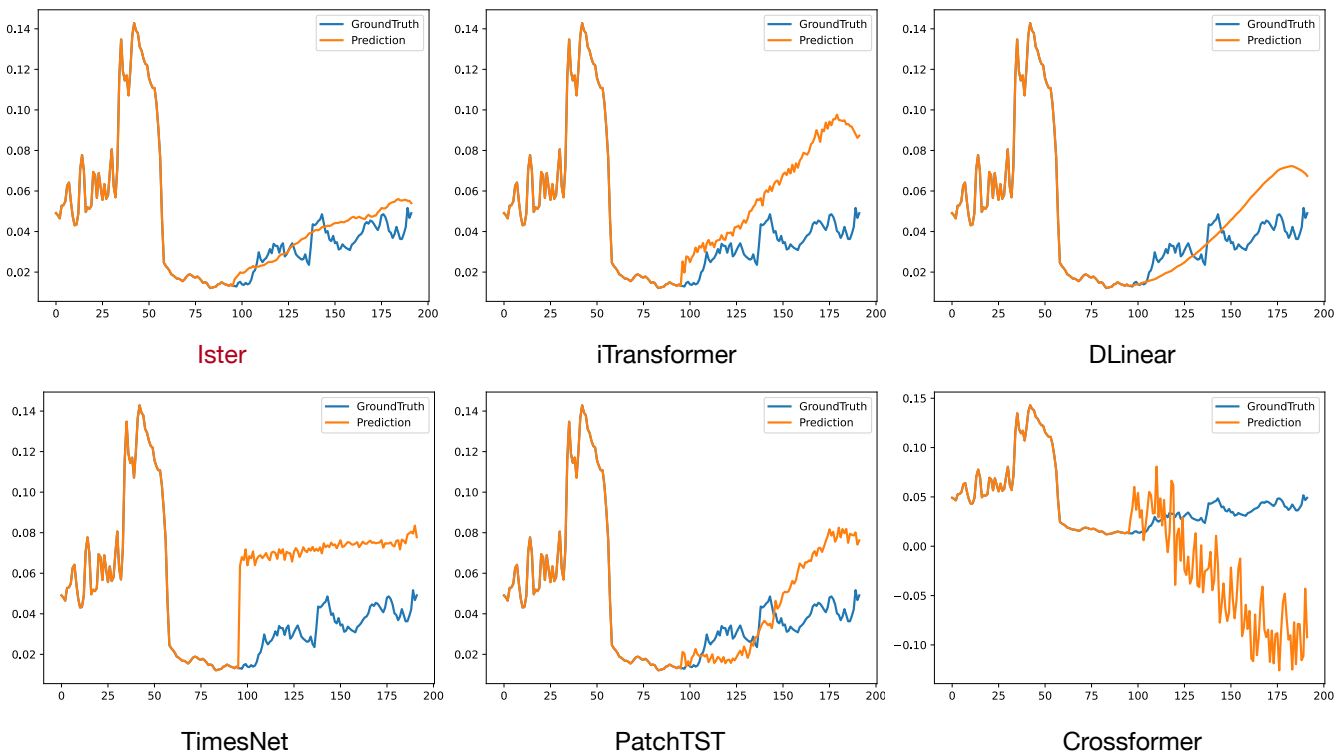


Figure 10: Visualization of input-96-predict-96 results on the Weather dataset.

## **E Full results**

### **E.1 Results of Forecasting Task (Table 8)**

### **E.2 Results of Ablations (Table 7)**

Model		iTransformer				PatchTST				Transformer			
Attention		FULL		DOT		FULL		DOT		FULL		DOT	
Metric		MSE	MAE	MSE	MAE	MSE	MAE	MSE	MAE	MSE	MAE	MSE	MAE
ECL	96	0.148	<b>0.240</b>	<b>0.147</b>	<b>0.240</b>	0.181	0.270	<b>0.168</b>	<b>0.266</b>	0.321	0.415	<b>0.254</b>	<b>0.349</b>
	192	0.165	<b>0.256</b>	<b>0.163</b>	<b>0.256</b>	0.187	0.275	<b>0.178</b>	<b>0.273</b>	0.358	0.439	<b>0.268</b>	<b>0.361</b>
	336	0.177	0.270	<b>0.174</b>	<b>0.268</b>	0.203	0.291	<b>0.198</b>	<b>0.293</b>	0.455	0.501	<b>0.274</b>	<b>0.366</b>
	720	0.228	0.313	<b>0.204</b>	<b>0.295</b>	0.245	0.325	<b>0.235</b>	<b>0.323</b>	0.524	0.549	<b>0.280</b>	<b>0.364</b>
	Avg	0.179	0.269	<b>0.172</b>	<b>0.264</b>	0.204	0.290	<b>0.194</b>	<b>0.288</b>	0.414	0.476	<b>0.269</b>	<b>0.360</b>
Promotion		-	-	4.0%	2.0%	-	-	5.0%	1.0%	-	-	35%	25%
Traffic	96	0.393	0.268	<b>0.382</b>	<b>0.261</b>	0.485	0.318	<b>0.423</b>	<b>0.279</b>	0.646	0.354	<b>0.642</b>	<b>0.347</b>
	192	0.411	0.276	<b>0.396</b>	<b>0.268</b>	0.487	0.315	<b>0.440</b>	<b>0.287</b>	0.661	0.364	<b>0.620</b>	<b>0.361</b>
	336	0.424	0.282	<b>0.406</b>	<b>0.273</b>	0.501	0.321	<b>0.453</b>	<b>0.293</b>	0.660	<b>0.360</b>	<b>0.646</b>	0.367
	720	0.459	0.301	<b>0.435</b>	<b>0.287</b>	0.536	0.338	<b>0.487</b>	<b>0.308</b>	<b>0.675</b>	0.368	<b>0.675</b>	<b>0.362</b>
	Avg	0.421	0.281	<b>0.404</b>	<b>0.272</b>	0.502	0.323	<b>0.450</b>	<b>0.291</b>	<b>0.660</b>	0.361	0.645	<b>0.359</b>
Promotion		-	-	4.1%	4.3%	-	-	11%	10%	-	-	2.3%	0.6%
PEMS08	12	0.083	0.186	<b>0.081</b>	<b>0.185</b>	0.168	0.232	<b>0.086</b>	<b>0.189</b>	0.209	0.237	<b>0.205</b>	<b>0.234</b>
	24	0.119	0.223	<b>0.118</b>	<b>0.220</b>	0.224	0.281	<b>0.138</b>	<b>0.239</b>	0.243	0.260	<b>0.228</b>	<b>0.256</b>
	48	0.191	0.277	<b>0.184</b>	<b>0.275</b>	0.321	0.354	<b>0.237</b>	<b>0.307</b>	0.270	0.294	<b>0.259</b>	<b>0.272</b>
	96	0.310	0.330	<b>0.294</b>	<b>0.322</b>	0.408	0.417	<b>0.315</b>	<b>0.320</b>	0.287	0.306	<b>0.275</b>	<b>0.291</b>
	Avg	0.175	0.254	<b>0.169</b>	<b>0.250</b>	0.280	0.321	<b>0.194</b>	<b>0.263</b>	0.252	0.274	<b>0.241</b>	<b>0.263</b>
Promotion		-	-	3.5%	1.6%	-	-	31%	19%	-	-	4.5%	4.0%

Table 7: We compared the performance of original *Multi-head self-attention* and *Dot-attention* for several different types (Channel-wise, Patch-wise and Point-wise) of Transformer models. The experimental results show that dot attention not only outperforms full attention in terms of time complexity, but also retains accuracy and even able to improve on some datasets.

Methods		Ister		iTransformer		DLinear		TimesNet		PatchTST		Crossformer		TiDE		SCINet		Stationary	
Metric		MSE	MAE	MSE	MAE	MSE	MAE	MSE	MAE	MSE	MAE	MSE	MAE	MSE	MAE	MSE	MAE	MSE	MAE
Traffic	96	<b>0.374</b>	<b>0.259</b>	<u>0.393</u>	<u>0.268</u>	0.648	0.396	0.599	0.314	0.485	0.318	0.511	0.266	0.805	0.493	0.788	0.499	0.612	0.338
	192	<b>0.386</b>	<b>0.265</b>	<u>0.411</u>	<u>0.276</u>	0.598	0.370	0.622	0.323	0.487	0.315	0.530	0.293	0.756	0.474	0.789	0.505	0.613	0.340
	336	<b>0.405</b>	<b>0.273</b>	<u>0.424</u>	<u>0.282</u>	0.605	0.373	0.632	0.332	0.501	0.321	0.558	0.305	0.762	0.477	0.797	0.508	0.618	0.328
	720	<b>0.432</b>	<b>0.285</b>	<u>0.459</u>	<u>0.301</u>	0.645	0.395	0.648	0.344	0.536	0.338	0.589	0.328	0.719	0.449	0.841	0.523	0.653	0.355
ETTh1	96	<b>0.377</b>	0.401	0.394	0.409	<u>0.382</u>	<b>0.395</b>	0.452	0.453	<u>0.386</u>	<u>0.398</u>	0.420	0.439	0.479	0.464	0.654	0.599	0.513	0.491
	192	0.436	0.429	0.448	0.440	<b>0.432</b>	<b>0.425</b>	0.498	0.477	<u>0.435</u>	<u>0.426</u>	0.540	0.519	0.525	0.492	0.719	0.631	0.534	0.504
	336	<b>0.460</b>	<b>0.449</b>	0.492	0.465	0.491	0.467	0.536	0.494	<u>0.479</u>	<u>0.450</u>	0.720	0.646	0.565	0.515	0.778	0.659	0.588	0.535
	720	<b>0.481</b>	<b>0.475</b>	0.520	0.503	0.526	0.517	0.555	0.516	<u>0.491</u>	<b>0.475</b>	0.808	0.690	0.594	0.558	0.836	0.699	0.643	0.616
ETTh2	96	<b>0.284</b>	0.341	0.299	0.349	0.339	0.393	0.331	0.369	0.290	<b>0.338</b>	0.846	0.634	0.400	0.440	0.707	0.621	0.476	0.458
	192	<b>0.355</b>	<b>0.385</b>	<u>0.381</u>	<u>0.399</u>	0.481	0.479	0.396	0.410	<u>0.382</u>	0.405	1.783	1.022	0.528	0.509	0.860	0.689	0.512	0.493
	336	<b>0.345</b>	<b>0.387</b>	<u>0.423</u>	<u>0.432</u>	0.590	0.540	0.452	0.450	<u>0.411</u>	<u>0.425</u>	2.650	1.405	0.643	0.571	1.000	0.744	0.552	0.551
	720	<b>0.412</b>	<b>0.436</b>	0.430	0.446	0.839	0.660	0.438	0.450	<u>0.422</u>	<u>0.443</u>	3.061	1.472	0.874	0.679	1.249	0.838	0.562	0.560
ETTm1	96	<b>0.323</b>	<b>0.361</b>	0.345	0.375	0.346	0.373	0.334	0.376	<u>0.329</u>	<u>0.365</u>	0.360	0.401	0.364	0.387	0.418	0.438	0.386	0.398
	192	<b>0.366</b>	<b>0.385</b>	0.391	0.399	0.381	0.391	0.404	0.410	<u>0.368</u>	<u>0.386</u>	0.402	0.440	0.398	0.404	0.439	0.450	0.459	0.444
	336	<b>0.399</b>	<b>0.410</b>	0.436	0.426	0.415	0.414	0.416	0.423	<u>0.400</u>	<b>0.410</b>	0.543	0.528	0.428	0.425	0.490	0.485	0.495	0.464
	720	<b>0.457</b>	<b>0.443</b>	0.504	0.465	0.473	0.451	0.497	0.466	<u>0.463</u>	<u>0.446</u>	1.073	0.794	0.487	0.461	0.595	0.550	0.585	0.516
ETTm2	96	<b>0.177</b>	<b>0.261</b>	<u>0.183</u>	0.265	0.193	0.292	0.189	0.266	<u>0.184</u>	<u>0.264</u>	0.270	0.356	0.207	0.305	0.286	0.377	0.192	0.274
	192	<b>0.243</b>	<b>0.304</b>	0.253	0.311	0.284	0.361	0.252	0.306	<u>0.246</u>	<u>0.306</u>	0.470	0.522	0.290	0.364	0.399	0.445	0.280	0.339
	336	<b>0.300</b>	<b>0.340</b>	0.312	0.350	0.382	0.429	0.322	0.349	<u>0.308</u>	<u>0.346</u>	1.165	0.759	0.377	0.422	0.637	0.591	0.334	0.361
	720	<b>0.396</b>	<b>0.395</b>	0.417	0.409	0.557	0.524	0.422	<u>0.407</u>	<u>0.404</u>	0.409	6.048	1.693	0.558	0.524	0.960	0.735	0.417	0.413
ECL	96	<b>0.138</b>	<b>0.234</b>	<u>0.148</u>	<b>0.240</b>	0.297	0.394	0.168	0.271	0.181	0.270	0.150	0.253	0.237	0.329	0.247	0.345	0.169	0.273
	192	<b>0.155</b>	<b>0.248</b>	<u>0.165</u>	<u>0.256</u>	0.299	0.397	0.190	0.292	0.187	0.275	0.166	0.267	0.236	0.330	0.257	0.355	0.182	0.286
	336	<b>0.172</b>	<b>0.266</b>	<u>0.177</u>	<u>0.270</u>	0.310	0.407	0.204	0.306	0.203	0.291	0.189	0.287	0.249	0.344	0.269	0.369	0.200	0.304
	720	<b>0.204</b>	<b>0.295</b>	<u>0.228</u>	<u>0.313</u>	0.343	0.432	0.272	0.353	0.245	0.325	0.231	0.318	0.284	0.373	0.299	0.390	0.222	0.321
Weather	96	<b>0.157</b>	<b>0.203</b>	0.173	<u>0.212</u>	0.195	0.254	<u>0.169</u>	0.219	0.180	0.220	0.174	0.239	0.202	0.261	0.221	0.306	0.173	0.223
	192	<b>0.206</b>	<b>0.248</b>	0.224	<u>0.256</u>	0.237	0.295	<u>0.226</u>	0.265	0.221	0.257	0.232	0.302	0.242	0.298	0.261	0.340	0.245	0.285
	336	<b>0.262</b>	<b>0.290</b>	0.280	0.299	0.281	0.331	0.281	0.303	0.279	<u>0.296</u>	<u>0.276</u>	0.340	0.287	0.335	0.309	0.378	0.321	0.338
	720	<u>0.347</u>	<b>0.345</b>	0.360	0.351	<b>0.345</b>	0.381	0.359	0.354	0.357	<u>0.350</u>	0.371	0.410	0.351	0.386	0.377	0.427	0.414	0.410
Exchange	96	<b>0.080</b>	<b>0.199</b>	0.088	0.209	0.098	0.232	0.105	0.235	<u>0.087</u>	<u>0.204</u>	0.256	0.367	0.106	0.232	0.267	0.396	0.131	0.257
	192	<b>0.173</b>	<b>0.296</b>	0.180	0.302	0.186	0.325	0.237	0.354	<u>0.176</u>	<u>0.298</u>	0.469	0.508	0.201	0.323	0.351	0.459	0.235	0.351
	336	0.318	0.407	0.362	0.440	0.340	0.446	0.362	0.437	<b>0.300</b>	<b>0.397</b>	1.267	0.882	0.380	0.446	1.324	0.853	0.393	0.456
	720	<u>0.837</u>	<u>0.689</u>	0.907	0.724	<b>0.746</b>	<b>0.662</b>	0.940	0.738	0.886	0.707	1.766	1.068	1.104	0.793	1.058	0.797	1.448	0.881
PEMS03	12	<b>0.065</b>	<b>0.170</b>	0.071	0.174	0.122	0.243	0.085	0.192	0.099	0.216	0.090	0.203	0.178	0.305	<u>0.066</u>	<u>0.172</u>	0.081	0.188
	24	<b>0.085</b>	<b>0.195</b>	0.093	0.201	0.201	0.317	0.118	0.223	0.142	0.259	0.121	0.240	0.257	0.371	<b>0.085</b>	<u>0.198</u>	0.105	0.214
	48	<b>0.119</b>	<b>0.232</b>	0.125	<u>0.236</u>	0.333	0.425	0.155	0.260	0.211	0.319	0.202	0.317	0.379	0.463	0.127	0.238	0.154	0.257
	96	<b>0.164</b>	<b>0.274</b>	<u>0.165</u>	<u>0.275</u>	0.457	0.515	0.228	0.317	0.269	0.370	0.262	0.367	0.490	0.539	0.178	0.287	0.247	0.336
PEMS04	12	<u>0.076</u>	<u>0.178</u>	0.078	0.183	0.148	0.272	0.087	0.195	0.105	0.224	0.098	0.218	0.219	0.340	<b>0.073</b>	<b>0.177</b>	0.088	0.196
	24	<u>0.091</u>	<u>0.198</u>	0.095	0.205	0.224	0.340	0.103	0.215	0.153	0.275	0.131	0.256	0.292	0.398	<b>0.084</b>	<b>0.193</b>	0.104	0.216
	48	<u>0.115</u>	<u>0.224</u>	0.120	0.233	0.355	0.437	0.136	0.250	0.229	0.339	0.205	0.326	0.409	0.478	<b>0.099</b>	<b>0.211</b>	0.137	0.251
	96	<u>0.143</u>	<u>0.252</u>	0.150	0.262	0.452	0.504	0.190	0.303	0.291	0.389	0.402	0.457	0.492	0.532	<b>0.114</b>	<b>0.227</b>	0.186	0.297
PEMS07	12	<b>0.059</b>	<b>0.156</b>	<u>0.067</u>	<u>0.165</u>	0.115	0.242	0.082	0.181	0.095	0.207	0.094	0.200	0.173	0.304	0.068	0.171	0.083	0.185
	24	<b>0.077</b>	<b>0.179</b>	<u>0.088</u>	<u>0.190</u>	0.210	0.329	0.101	0.204	0.150	0.262	0.139	0.247	0.271	0.383	0.119	0.225	0.102	0.207
	48	<b>0.102</b>	<b>0.206</b>	<u>0.110</u>	<u>0.215</u>	0.398	0.458	0.134	0.238	0.253	0.340	0.311	0.369	0.446	0.495	0.149	0.237	0.136	0.240
	96	<b>0.130</b>	<b>0.231</b>	<u>0.139</u>	<u>0.245</u>	0.594	0.553	0.181	0.279	0.346	0.404	0.396	0.442	0.628	0.577	0.141	0.234	0.187	0.287
PEMS08	12	<b>0.076</b>	<b>0.176</b>	0.079	<u>0.182</u>	0.154	0.276	0.112	0.212	0.168	0.232	0.165	0.214	0.227	0.343	0.087	0.184	0.109	0.207
	24	<b>0.107</b>	<b>0.208</b>	<u>0.115</u>	<u>0.219</u>	0.248	0.353	0.141	0.238	0.224	0.281	0.215	0.260	0.318	0.409	0.122	0.221	0.140	0.236
	48	<b>0.168</b>	<u>0.258</u>	<u>0.186</u>	<b>0.235</b>	0.440	0.470	0.198	0.283	0.321	0.354	0.315	0.355	0.497	0.510	0.189	0.270	0.211	0.294
	96	<b>0.195</b>	<b>0.264</b>	<u>0.221</u>	<u>0.267</u>	0.674	0.565	0.320	0.351	0.408	0.417	0.377	0.397	0.721	0.592	0.236	0.300	0.345	0.367
1 <sup>st</sup> Count		<b>78</b>		2		6		1		5		1		0		<u>9</u>		0	

Table 8: Full results of the Forecasting Task. We compare competitive models in Long-term Forecasting Task under different prediction lengths following the setting of original papers. The input sequence length is set to 96 for all baselines. The best results are in **bold** and the second best results are underlined.